Triangular and Kagome Antiferromagnets with a Strong Easy-Axis Anisotropy

Arnab Sen,[1] Fa Wang,[2] Kedar Damle,[1] and R. Moessner[3]

[1]*Department of Theoretical Physics, Tata Institute of Fundamental Research, Homi Bhabha Road, Mumbai 400005, India*
[2]*Department of Physics, University of California, Berkeley, California 64720, USA*
[3]*Max-Planck-Institut für Physik komplexer Systeme, 01187 Dresden, Germany*

(Received 13 November 2008; published 2 June 2009)

We consider $S > 3/2$ kagome and triangular lattice magnets with strong easy-axis single-ion anisotropy D and antiferromagnetic exchange J. When $D \gg J$, the low energy states selected by the anisotropy map onto configurations of the corresponding classical Ising antiferromagnet. Subleading $O(J^3S/D^2)$ multispin interaction arising from the transverse quantum dynamics makes the low-temperature behavior very different from the well-known classical case: The kagome magnet goes into a semiclassical spin-liquid state with distinctive and unusual short-range correlations below a crossover temperature $T^* \approx 0.08J^3S/D^2$, while the triangular magnet undergoes a first-order transition at $T_c \approx 0.1J^3S/D^2$ to an orientationally ordered collinear state that gives rise to a novel zero-magnetization plateau for small magnetic fields along the easy axis. Possible experimental implications are also discussed.

DOI: 10.1103/PhysRevLett.102.227001 PACS numbers: 75.50.Ee, 71.55.Jv, 74.20.Mn

Introduction.—Well-formed magnetic moments (''spins'') in insulators often display dominant short-range exchange interactions [1], which result in sharply defined transitions from high-temperature paramagnetic behavior to low-temperature magnetic order, the nature of which can usually be understood in terms of the unique minimum of the classical exchange energy. However, in some cases, the leading exchange interactions compete with each other due to the geometry of the lattice. Such *geometrically frustrated* systems often have many local minima in their classical energy landscape, or even a *macroscopic* number of inequivalent classical ground states, resulting in a wide crossover regime with cooperative paramagnetic behavior at intermediate temperatures below the exchange energy scale [2].

In most cases which display a cooperative paramagnetic regime, quantum fluctuations and subleading interactions eventually do lead to an (often complex) ordered state at still lower temperature. Systems with spins on the kagome lattice [Fig. 1(a)] provide many experimental examples of this physics [3–5]. In other frustrated magnets, e.g., in the $S = 1/2$ kagome lattice magnet *herbertsmithite* [6], there is no tendency of the spins to form an ordered arrangement even at the lowest temperatures accessible to experiment. Such systems provide possible realizations of so-called spin-liquid states, which have been the subject of sustained theoretical activity [7] going back to the work of Fazekas and Anderson [8].

Even when the classical energetics does pick a unique ground state spin configuration, this ordering can be particularly vulnerable to the effects of quantum fluctuations. Triangular lattice [Fig. 1(b)] antiferromagnets with nearest-neighbor *Heisenberg exchange* couplings, which are isotropic in spin space, provide a well-known example, with the classical coplanar 120° ordered state surviving the effects of quantum fluctuations down to $S = 1/2$, but with a significantly reduced ordered moment [9].

Much of the theoretical work [7] has focused on the challenging case of spin-1/2 moments with Heisenberg exchange interactions. In the opposite Ising limit, in which the exchange interactions only couple one component of neighboring $S = 1/2$ moments on the triangular or kagome lattice, there are no quantum fluctuations. These frustrated Ising models on the triangular and kagome lattices have been of interest in statistical mechanics for over half a century, and are known to have a macroscopic degeneracy of inequivalent classical ground states that results in cooperative paramagnetic behavior all the way down to $T = 0$ [10] on both lattices—indeed, the cooperative paramagnetic state of these Ising models provides the standard paradigm for the effects of frustration at the classical level.

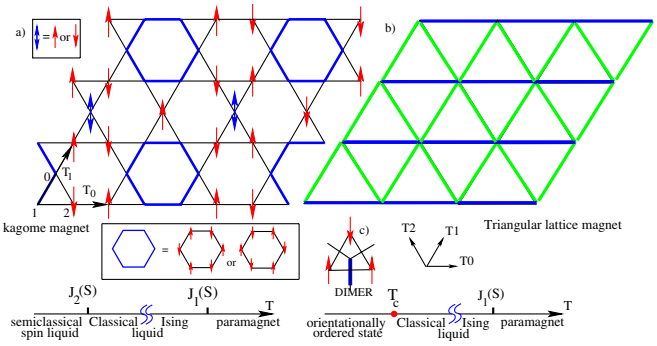

FIG. 1 (color online). (a) The kagome lattice (with $L_x = 4$, $L_y = 3$), and a macroscopic entropy ensemble of partially ordered states that simultaneously minimizes J_1 and J_2 on it. (b) The triangular lattice (with $L_x = L_y = 4$) and its orientationally ordered state: The average Ising exchange energy of the dark (blue) bonds is lower than that of the light (green) bonds. (c) Mapping of Ising spins to dimers on the dual lattice.

Motivation.—Such ''Ising spins'' can and do actually arise in experiments when $S \geq 1$ moments have a strong easy-axis single-ion anisotropy D in addition to the usual isotropic exchange coupling J in their effective Hamiltonian. When D is large, each spin has projection $\pm S$ along its easy axis, thus mimicking a two-state Ising system with interactions arising from ''longitudinal'' components of J along the easy axis. However, such Ising spins are also influenced by quantum fluctuations arising from the transverse components of the exchange coupling. The question then arises: Can these lead to low-temperature behavior qualitatively different from the well-known cooperative paramagnetic state of the corresponding classical Ising model?

Results.—We provide a unified account of the low-temperature properties of all such $S > 3/2$ triangular and kagome magnets with a common easy axis z for all spins:

$$H = J\sum_{\langle ij\rangle} \vec{S}_i \cdot \vec{S}_j - D\sum_i (S_i^z)^2, \tag{1}$$

and demonstrate that this question has interesting answers [11]: We find that such easy-axis magnets on the kagome lattice *do not* develop any long-range order down to very low temperature, and are thus good examples of spin-liquid behavior in a system of quantum spins. In the intermediate temperature range $T^* < T \ll JS^2$ (where $T^* \approx 0.08J^3S/D^2$ is a crossover temperature), the system is well described by the classical cooperative Ising paramagnet mentioned earlier. Below T^*, virtual quantum fluctuations dominate, leading to a qualitatively different ''semiclassical'' spin-liquid regime in which the structure factor of the spins encodes distinctive short-ranged correlations. In sharp contrast to this, triangular lattice magnets undergo an abrupt first-order transition at $T_c \approx 0.1J^3S/D^2$ from the intermediate temperature classical cooperative Ising paramagnet to an unusual orientationally ordered collinear state which gives rise to a *zero-magnetization plateau* over a range of small magnetic fields along the easy axis.

Our kagome results are of experimental relevance for the kagome antiferromagnet Nd-langasite that does not exhibit any magnetic order down to 50 mK [12,13], although the Nd^{3+} spins (that carry a total angular momentum quantum number $J_{\rm ion} = 9/2$) interact with nearest neighbors on the kagome lattice with an isotropic antiferromagnetic exchange coupling $J \approx 1.5$ K in the presence of a strong single-ion anisotropy term $D \approx 10$ K [14] that picks out the crystallographic c axis as the common easy axis of all the spins [15].

Effective Hamiltonian.—When D dominates over J, the leading D term picks *collinear spin states* that can be described by Ising pseudospin variables σ: $S_i^z = \sigma_i S$, with $\sigma_i = \pm 1$. The low energy physics in this regime is then best described in terms of an effective Hamiltonian $\mathcal{H}$ that encodes the splitting of this degenerate Ising subspace; this physics is thus different from that of the intermediate anisotropy regime, in which noncollinear configurations dominate at low temperatures and fields, leading to a sequence of noncollinear phases [16,17].

To (leading) $O(J^3/D^2)$, an elementary perturbative calculation (similar to but simpler than degenerate perturbation theory analyses of magnetization plateaus in finite field [18,19]) gives the effective Hamiltonian

$$\mathcal{H} = J_1\sum_{\langle ij\rangle} \sigma_i\sigma_j - J_2\sum_{\langle ij\rangle} \frac{1-\sigma_i\sigma_j}{2}(\sigma_i H_i + \sigma_j H_j), \tag{2}$$

where $J_1 = JS^2$, $J_2 = \frac{S^3J^3}{4D^2(2S-1)^2}$, and the *exchange field* $H_i \equiv \sum_j \Gamma_{ij}\sigma_j$ with $\Gamma_{ij} = 1$ for nearest neighbors and zero otherwise. In the above, the first term corresponds to the leading effect of the z component of the spin exchange, while the second term arises from the effects of *virtual* quantum transitions of pairs of antialigned spins out of the low energy Ising subspace. An additional $O(J^{2S}/D^{2S-1})$ pseudospin exchange term (not displayed above), representing real quantum transitions, is subdominant for $S > 3/2$, making the physics of these high-spin magnets quite different from the $S = 1$ case where real quantum transitions dominate, leading to spin-nematic order [20].

Classical Ising regime.—Below the exchange energy scale J_1, the system crosses over to an intermediate temperature regime $J_2 \ll T \ll J_1$ whose physics is controlled by the ground states of the corresponding classical Ising antiferromagnet. In these ground states each triangle has exactly one frustrated bond (connecting a pair of aligned spins). This ''minimally frustrated'' ensemble of states has a residual entropy of $0.502k_B$ ($0.323k_B$) per spin in the kagome (triangular) case [10]. This macroscopic entropy ensemble of ground states can be conveniently represented by dimer configurations on the dice (honeycomb) lattice dual to the kagome (triangular) lattice, wherein a dimer is placed on every link of the dual lattice that intersects a frustrated bond of the original spin configuration [Fig. 1(c)]. In the kagome case, spin correlations averaged over this ground state ensemble are very short ranged [10], yielding a completely featureless spin structure factor. On the triangular lattice, spin correlations at the three-sublattice wave vector build up at low temperature, but there is no long-range order. This intermediate temperature regime $J_2 \ll T \ll J_1$ in both cases is thus a classical cooperative Ising paramagnet.

$T \lesssim J_2$.—Next, we note that the minimum frustration condition immediately implies that $\sum_{\langle ij\rangle}(\sigma_i\sigma_j - 1) \times (\sigma_i H_i + \sigma_j H_j)/2 = \sum_i (\sigma_i H_i)^2/2$ (apart from an additive constant). This allows us to write the projected multispin interaction J_2 [Eq. (2)] as an interaction between dimers [Fig. 1(c)]:

$$H_D = 2J_2\sum_P n^2 |nP\rangle\langle nP|, \tag{3}$$

where $|nP\rangle$ denotes elementary plaquettes with n dimers on their perimeter. Somewhat remarkably, the *form* of this

interaction remains the same for all $S > 3/2$, and all the S dependence is in the prefactor $J_2(S)$.

This potential energy H_D is minimized on the dice lattice (dual to kagome lattice) when elementary plaquettes with no dimers on their perimeter are disallowed. In spin language, it implies that no spin should be the minority spin of both the triangles to which it belongs. We have investigated the set of configurations that satisfy this constraint in some detail, and find that it is possible to construct a large subset of states (i.e., with macroscopic entropy) satisfying the rule, and all related to each other by local spin flips [Fig. 1(a)]. This construction immediately provides a lower bound of $k_B \ln(2)/6$ per site on the entropy of the ground states of $\mathcal{H}_D$. On the honeycomb lattice (dual to triangular lattice), H_D is minimized by dimer configurations in which all hexagons have precisely two dimers on their perimeter. Detailed analysis reveals that the ground state entropy in this case is subextensive unlike in the kagome case. These bounds on the ground state degeneracy leave open the possibility of low-temperature entropic ordering within the ground state manifold, and below we present results of detailed Monte Carlo simulations of H_D to shed light on this possibility. (Our numerics relies on an efficient generalization of the loop algorithm of Refs. [21,22].)

Orientationally ordered state on triangular lattice.—We find that below a critical temperature $T_c \approx 1.67 J_2(S)$, the system enters an *orientationally ordered state* in which the mean Ising exchange energy on a link of the triangular lattice depends only on its orientation.

This is seen [Fig. 2(a)] in the behavior of the orientational order parameter $\Phi = \sum_p - B_p e^{2p\pi i/3}$, where B_p denotes the average of the Ising exchange energy $\sigma_i \sigma_j$ on all links $\langle ij \rangle$ of the pth orientation ($p = 0, 1, 2$) on the triangular lattice [Fig. 1(b)]. From the double peak nature of the histogram of the order parameter at the transition, we see that the transition has a first-order character [Fig. 2(b)]. In such an orientationally ordered state, the Ising pseudospins are antiferromagnetically arranged in parallel rows oriented along one spontaneously chosen principal direction of the triangular lattice. Each such row can be in one of two internal states corresponding to the two antiferromagnetic arrangements of σ on that row, and we probe possible relative ordering of these internal states by monitoring the structure factor of the Ising spins σ. (Any long-range order in these internal states would give rise to a Bragg peak in this structure factor, while the absence of any observed Bragg peaks would imply either a random *glassy* pattern of internal states or rapidly fluctuating internal states.)

As is clear from Fig. 2(c), there is no long-range order in the internal states of the antiferromagnetic rows. In fully equilibrated simulations that employ efficient nonlocal multispin updates, we find that the antiferromagnetic rows fluctuate freely between their two allowed internal states. With realistic single-spin flip or spin-exchange dynamics, we find that the antiferromagnetic rows freeze into

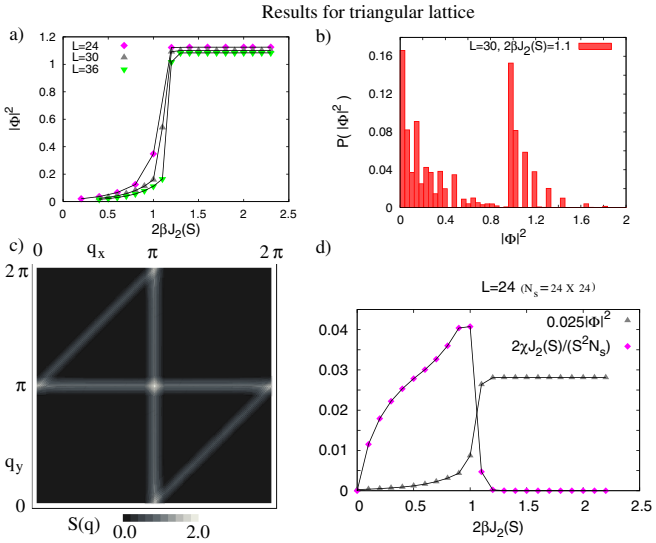

FIG. 2 (color online). (a) Temperature dependence of the orientational order parameter Φ. (b) The double peak in the histogram of Φ provides a clear signature of a first-order jump in Φ at the transition. (c) Contour plot of the equal time spin structure factor for size $L = 24$ at $2\beta J_2(S) = 2.2$. The Bragg lines with enhanced scattering are the signature of the orientational order. (d) The magnetic susceptibility behavior of a $N_s \equiv L^2$ site system across the transition.

a random glassy pattern of internal states as we approach T_c. (Similar glassy behavior due to formation of extended structures has been discussed earlier [19,23].)

Another interesting aspect of this orientationally ordered state follows from the exponential suppression $[O(e^{-J_2(S)/T})]$ of the total easy-axis magnetization $\langle M_{\rm tot} \rangle$ and the corresponding susceptibility χ [Fig. 2(d)], since perfect orientational order implies zero magnetization for each individual antiferromagnetic row of spins, and defects cost energy of order $J_2(S)$. As this ordered state is stable to small magnetic fields at which the corresponding Zeeman energy is small compared to the multispin interaction energy J_2, this implies the presence of a low-temperature *zero-magnetization plateau* that extends for a range of magnetic fields $0 < |B| < B_c \sim J^3/D^2$.

Semiclassical spin liquid on kagome lattice.—From numerical simulations on $L_x = L_y = L$ size systems using this algorithm (with L ranging from 10 to 60), we see no evidence at all of any phase transition as we lower the temperature to access the $T \to 0$ limit. This is evident from the behavior of the specific heat per site, which saturates very quickly with system size, and does not show any singularity in the thermodynamic limit [Fig. 3(a)]. In addition, the spin-spin correlators as well as the bond-energy correlators show no long-range order at any wave vector down to the lowest temperatures we study [Fig. 3(b)]. The system thus remains in a short-ranged ordered spin-liquid state down to the lowest temperatures, in sharp contrast to the long-range order that is expected to develop at low temperature in the presence of magnetic fields $B \sim JS$ along the easy axis [19].

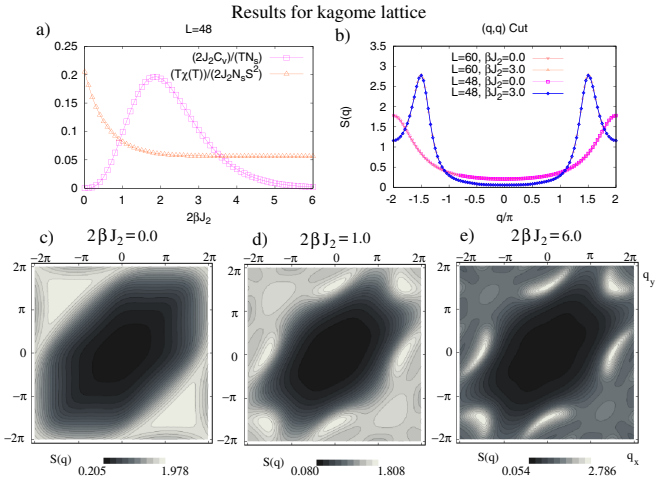

FIG. 3 (color online). (a) Specific heat C_v and the uniform susceptibility χ in the crossover region to the semiclassical spin liquid. (b) $S(\vec{q})$ along a $q_x = q_y$ cut for system sizes $L = 48, 60$, and inverse temperatures $\beta J_2 = 0.0, 3.0$. (c)–(e) Spin structure factor $S(\vec{q})$ shown for three different temperatures, showing crossover to semiclassical spin-liquid regime.

Although there is no phase transition, the low-temperature liquid is quite different from the classical cooperative Ising paramagnet. This *crossover* to a distinct semiclassical spin-liquid regime [Fig. 3(a)] is evident in the temperature dependence of the specific heat per site C_v/N_s, and the magnetization fluctuations $T\chi$. The C_v vs T curve shows a distinct but nonsingular peak at $T^* \approx 1.3J_2$ that reflects the loss of entropy during this crossover from the cooperative Ising paramagnet to the low-temperature limit in which the configurations sampled predominantly obey the minimum J_2 constraint (the C_v/T data give an estimate of $0.32k_B$ per spin for the residual entropy of the semiclassical spin liquid).

A clear signature of this crossover to the semiclassical spin liquid below T^* is provided by the spin structure factor (probed in neutron scattering experiments): $S(\vec{q}) = |S_0(\vec{q}) \exp(iq_y/2) + S_1(\vec{q}) + S_2(\vec{q}) \exp(iq_x/2)|^2$, where $S_\alpha(\vec{q})$ is the Fourier transform of the spin density on sublattice α of the kagome lattice [Fig. 1(a)] and q_x (q_y) refers to the projection of $\vec{q}$ onto lattice direction T_0 (T_1) measured in units of inverse Bravais lattice spacing. $S(\vec{q})$ evolves continuously from being quite featureless in the classical cooperative Ising regime $T^* \ll T \ll J_1$ to developing characteristic crescents of high intensity diffuse scattering in the low-temperature semiclassical spin-liquid regime $T \ll T^*$, with precursors of these features being already present at $T \sim 2T^*$ [Figs. 3(c)–3(e)]. As qualitative features, such crescents should be relatively robust to smearing due to, e.g., crystal imperfections, providing an experimental fingerprint of the semiclassical spin liquid akin to the singular ''pinch-point'' signatures of the spin-ice phase in $Dy_2Ti_2O_7$ [24].

Using [14] $J \approx 1.5$ K and $D \approx 10$ K, we obtain $T^* \approx 16$ mK, and we thus expect a simple classical Ising description of the spin structure factor to work fairly well at $T > 32$ mK—this is consistent with the nearly featureless diffuse scattering seen in neutron scattering experiments above 50 mK [12,13]. We thus hope that our results might motivate lower-T studies that probe the crossover to the semiclassical spin-liquid state.

We thank F. Bert and D. Dhar for useful discussion and correspondence, and A. Vishwanath for collaboration on related work. We acknowledge computational resources at TIFR and support from DST SR/S2/RJN-25/2006 (K. D.).

[1] J. B. Goodenough, *Magnetism and the Chemical Bond* (InterScience-Wiley, New York, 1963).
[2] R. Moessner, Can. J. Phys. **79**, 1283 (2001).
[3] M. Kenzelmann *et al.*, Phys. Rev. B **74**, 014429 (2006).
[4] I. S. Hagemann *et al.*, Phys. Rev. Lett. **86**, 894 (2001); D. Bono *et al.*, Phys. Rev. Lett. **92**, 217202 (2004).
[5] K. Matan *et al.*, Phys. Rev. Lett. **96**, 247201 (2006); T. Yildirim and A. B. Harris, Phys. Rev. B **73**, 214446 (2006).
[6] J. S. Helton *et al.*, Phys. Rev. Lett. **98**, 107204 (2007).
[7] G. Misguich and C. Lhuillier, in *Frustrated Spin Systems*, edited by H. T. Diep (World Scientific, Singapore, 2005).
[8] P. Fazekas and P. W. Anderson, Philos. Mag. **30**, 423 (1974).
[9] L. Capriotti, A. E. Trumper, and S. Sorella, Phys. Rev. Lett. **82**, 3899 (1999), and references therein.
[10] R. Liebmann, *Statistical Mechanics of Periodic Frustrated Ising Systems* (Springer, Berlin, 1986).
[11] For insightful discussions of similar questions in some Heisenberg magnets, see O. Tchernyshyov, J. Phys. Condens. Matter **16**, S709 (2004); U. Hizi and C. L. Henley, Phys. Rev. B **73**, 054403 (2006).
[12] J. Robert *et al.*, Phys. Rev. Lett. **96**, 197205 (2006).
[13] H. D. Zhou *et al.*, Phys. Rev. Lett. **99**, 236401 (2007).
[14] A. Zorko *et al.*, Phys. Rev. Lett. **100**, 147201 (2008).
[15] P. Bordet *et al.*, J. Phys. Condens. Matter **18**, 5147 (2006).
[16] S. Miyashita, J. Phys. Soc. Jpn. **55**, 3605 (1986).
[17] P. E. Melchy and M. E. Zhitomirksy, arXiv:0812.3574.
[18] D. L. Bergman, R. Shindou, G. A. Fiete, and L. Balents, Phys. Rev. B **75**, 094403 (2007).
[19] A. Sen, K. Damle, and A. Vishwanath, Phys. Rev. Lett. **100**, 097202 (2008).
[20] K. Damle and T. Senthil, Phys. Rev. Lett. **97**, 067202 (2006); K. Damle, Physica (Amsterdam) **384A**, 28 (2007).
[21] A. W. Sandvik and R. Moessner, Phys. Rev. B **73**, 144504 (2006).
[22] F. Alet *et al.*, Phys. Rev. Lett. **94**, 235702 (2005).
[23] D. Das, J. Kondev, and B. Chakraborty, Europhys. Lett. **61**, 506 (2003).
[24] R. Moessner and A. P. Ramirez, Phys. Today **59**, No. 2, 24 (2006); T. Fennell *et al.*, Nature Phys. **3**, 566 (2007).